2D Investigation of Seabed Stress Around Subsea Pipelines

Martin Kalkhoven

Dr Jeremy Leggoe
School of Mechanical and Chemical Engineering

Terry Griffiths
CEED Client: J P Kenny

Abstract

Local scour around subsea pipelines has been observed to lead to self-burial and may be exploited as a cost effective alternative to traditional pipeline stability measures. A major forcing mechanism of scour and sediment transport is seabed shear stress which is investigated in this project through computational fluid dynamics (CFD) numerical modelling of varying geometric parameters and wave & current conditions. The seabed shear stress profiles generated can be used for a better understanding of different stages of scour and self burial. Results to date indicate a combination of waves and currents significantly increase seabed shear stress as does increasing the seabed grain size. These are likely to increase sediment transport as well as scour rates. Varying water depth and wave dimensions had little effect on seabed shear stress in the range tested to date. This investigation builds on two previous CEED projects from 2010 and 2011.

1. Introduction

Subsea pipelines used to export hydrocarbon fluids to onshore processing facilities can periodically be exposed to extreme weather conditions, generating significant hydrodynamic forces. Traditional approaches to pipeline stability in these extreme conditions have resulted in few failure cases but are very costly to implement. Field observations on some existing pipelines indicate that local scour around pipes laid on an erodible seabed can lead to self burial (Li & Cheng, 2001). This significantly increases the lateral resistance of the pipe and may be exploited as a cost effective alternative to rock dumping or trenching to ensure pipeline stability.

The work of Sumer et al (2001) and others showed that piping is the dominant cause for the initiation of scour below a pipeline for both current and wave cases. In a flow, a pipeline on an erodible porous seabed develops a pressure gradient from upstream to the downstream side. This induces a seepage flow through the underlying sediments and hence a force being exerted on the sediment grains. When the pressure gradient exceeds the floatation gradient of the grains, a mixture of water and sediment breaks through and scour is initiated. Scour may break through at several points and propagate in both directions along the pipe axis.

Developing scour holes are interrupted by stretches of supporting soil called span shoulders which may continue to erode, resulting in more pipe weight being exerted on reducing span shoulder length. This continues until the bearing capacity of the soil is exceeded, with the soil failing in general shear failure and sliding outwards. The pipeline sinks to the bottom of the scour hole with no more sediment passing underneath. Suspended sediment, transported by the flow, continues to be deposited on either side of the pipe leading to partial self-burial.

Soulsby (1997) shows that sediment transport occurs when the Shields parameter exceeds a critical value which is dependent on seabed shear stress. Cheng et al (2009) found that scour propagation velocity increases with increasing Shields parameter but decreases with increasing pipe embedment. Sumer & Fredsøe (1991) measured bed shear stress during the course of a half period of oscillatory flow for a pipe resting on a flat seabed and above a flat seabed with a 0.05 pipe diameter gap. A dramatic change in seabed shear stress patterns was observed once there was a pipe gap and hence would have a direct effect on sediment transport and deposition. The dramatic change in seabed shear stress is supported by the work of Xu (2010) and Shen (2011).

The J.P.Kenny has developed a novel two dimensional pipe-soil-fluid (PSF) interaction model which incorporates sediment transport and scour (Griffiths, 2012). The PSF model has been designed to minimise computational costs compared to continuum soil FEA and 3D RANS-based CFD approaches and will enable it to be used for practicle pipeline stability analysis.

A major output of this project for the J.P.Kenny is a set of seabed shear stress profiles of arbitrary seabed-with-pipe sections. These are generated by running a range of 2D CFD numerical simulations with varying geometric parameters and wave & current conditions. The seabed shear stress profiles are converted into "local velocity" values which are then used to model sediment transport in the client's pipe-soil-fluid (PSF) interaction model. This will build on two previous studies of the same topic (Xu,2010 and Shen, 2011).

2. Numerical Method and Computational Domain

The 2D numerical simulations were performed using ANSYS Fluent 13.0 SP2 software which is a CFD finite element solver for the governing Reynolds Averaged Navier-Stokes equations. The turbulence closure model used was the two equation eddy viscosity, SST k-ω model and had previously been validated by the work of Shen (2011).

2.1 Computational Domain and Boundary Conditions

The geometric size of the computational domain and the boundary conditions used for all the simulations are shown in Figure 1. Each domain consisted of a cylindrical cross section representing a pipeline and a flow field of 100 pipe diameters in length up and down stream of the pipe. Domain height was fiteen pipe diameters although actual water depth (d) was at least 40m. By varying the parameters, L_{berm} , Z_{berm} , Z_{soil} , Z_{pipe} and *Gap*, different seabed and pipe profiles representing various stages of scour and self burial could be simulated.

The boundary conditions of the domain's side and top flow velocity inlets were prescribed by a common set of new user defined functions (UDFs) for horizontal and vertical velocity components (U_x & U_y), turbulent kinetic energy (k) and specific dissipation rate (ω). The pressure at the outlet boundary condition was set to equal zero however for backflow, velocity was set to match that of the neighbouring cells and use the common UDFs for k and ω. The wall/fluid (seabed and pipe surface) boundary conditions were set as no-slip with U_x & U_y=0.

The new UDFs were developed by starting with straight Airy Linear Wave Theory functions for the wave component of U_x & U_y and a logarithmic profile for the current component. For k and ω, the UDFs of Shen(2011) were used as a starting point. These initial UDFs were run in metocean numerical simulations for the equivalent of eleven wave cycles with empty

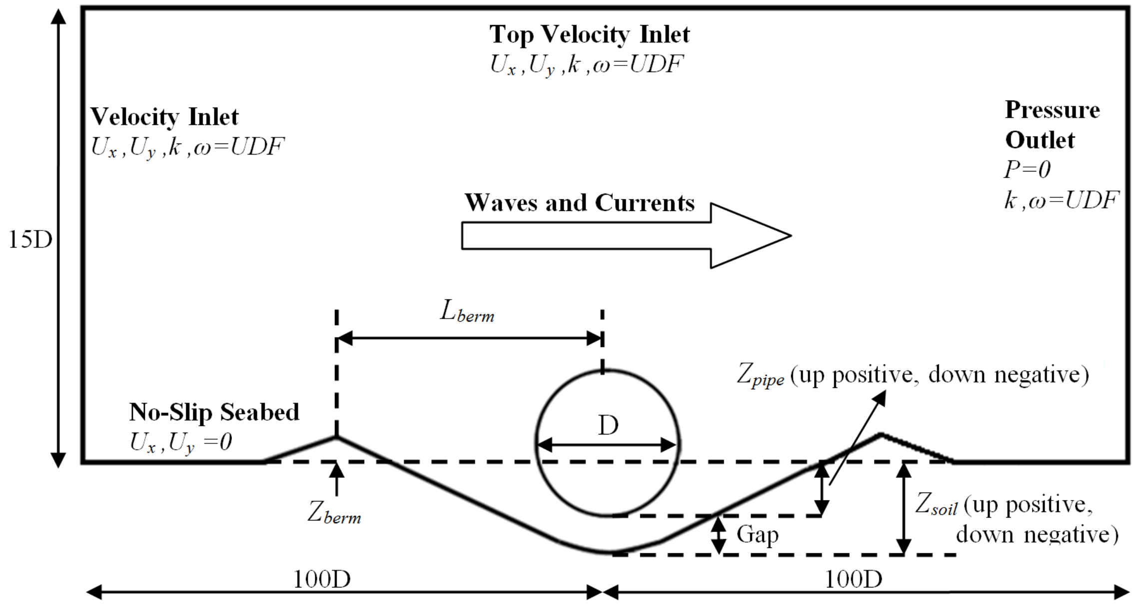

Figure 1 Computational domain geometric size and boundary conditions

domains and a flat seabed. Velocity, k and ω profiles were extracted at the centre of the domain and the UDFs modified to curve fit this test data. This resulted in continuous velocity functions and new polynomial and blended exponential functions for k and ω respectively.

2.2 Computational Meshing

The meshed geometries used in the early part of this project were those validated by Xu (2010) and Shen (2011). All new mesh geometries use the same four-node quadrilateral element structure as illustrated in Figure 2. and have yet to be validated for mesh independence. This will be achieved by running numerical simulations of the same domain geometry with increasing mesh densities until a there is no significant change in the seabed shear stress profiles.

Figure 2 a) Meshed computational domain, b) Close-up of area around pipe. Note the increasing mesh density towards wall boundaries.

3. Results and Discussion

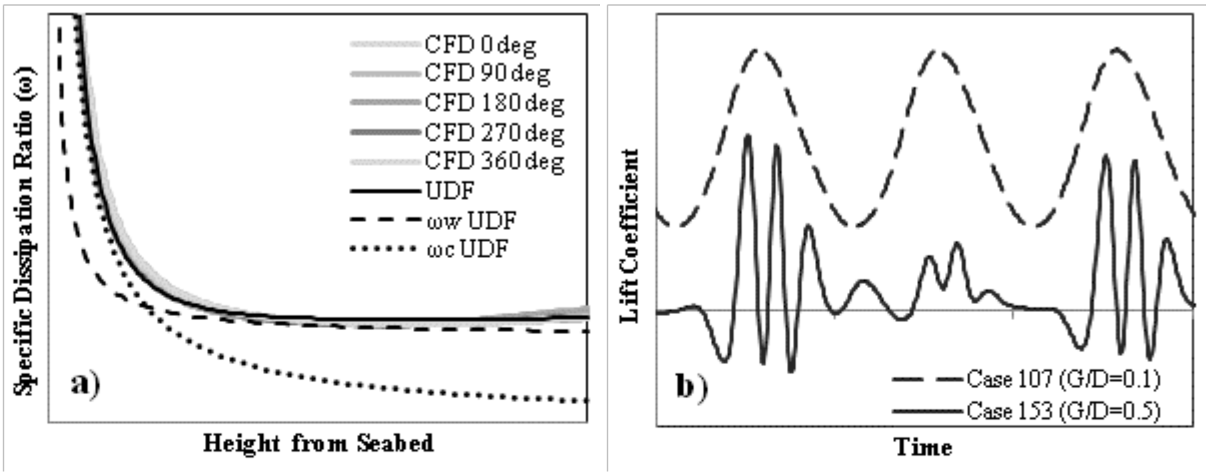

Figure 3 a) Curve fitting specific dissipation rate UDF against CFD test data, b) Lift coefficients of top of pipe from two similar case simulations under same conditions only varying normalised pipe to seabed gap

The results of the metocean numerical simulations with empty domains were used to optimise the UDF input functions and ensured a fully developed flow was used for each seabed with pipe simulation. In Figure 3a), the solid grey lines show the CFD specific dissipation rate (ω) profiles from the centre of an empty domain using a combined 1m/s steady current and 1m/s maximum wave velocity. The two dashed lines show individual exponential functions for a 1m/s wave and a 1m/s steady current respectively. These two functions were blended as a function of height from seabed to form the UDF input function for ω, as shown by the solid black line. This process was repeated for varying velocity combinations and the UDF function constants varied accordingly. The same approach was used for U_x , U_y and k UDFs.

An observation of the metocean simulations was that small errors in the U_y UDF had a huge effect on all velocity and turbulence profiles. This can be explained by the fact that the U_y boundary condition input dominates the top velocity inlet which is many times larger than the side velocity inlet, which is dominated by U_x. Also there is only a small domain height in which to develop the U_y flow component compared to the U_x component. It was found that the least error occurred with an unmodified Airey Linear Wave Theory function for the wave component of U_y.

The plots in Figure 3b) are of the lift coefficient (C_L) of the top of a pipe over three wave cycles, for two separate simulations. Both cases were of a pipe above a flat seabed but with different gap ratios (*Gap*/pipe diameter). Boundary conditions were the same except Case 107 had a slightly higher current velocity, which explains why the plot had a slightly higher average C_L. Case 107 had a G/D = 0.1 and displayed a regular sinusoidal C_L profile that follows the changes in wave velocity. Case 153 had a G/D = 0.5 and displayed an irregular C_L profile. This can be explained by vortex shedding which is confirmed by the Strouhal number of the shedding frequency, St =0.208. For Re > 1000 the dimensionless vortex shedding frequency is expressed as a Strouhal number, $St = fD/V$ and is approximately equal to 0.21. Kazeminezhad et al (2010) observed that vortex shedding does not occur with gap ratios G/D< 0.2 which correlates to Cases 107 & 153 and further validating the UDFs.

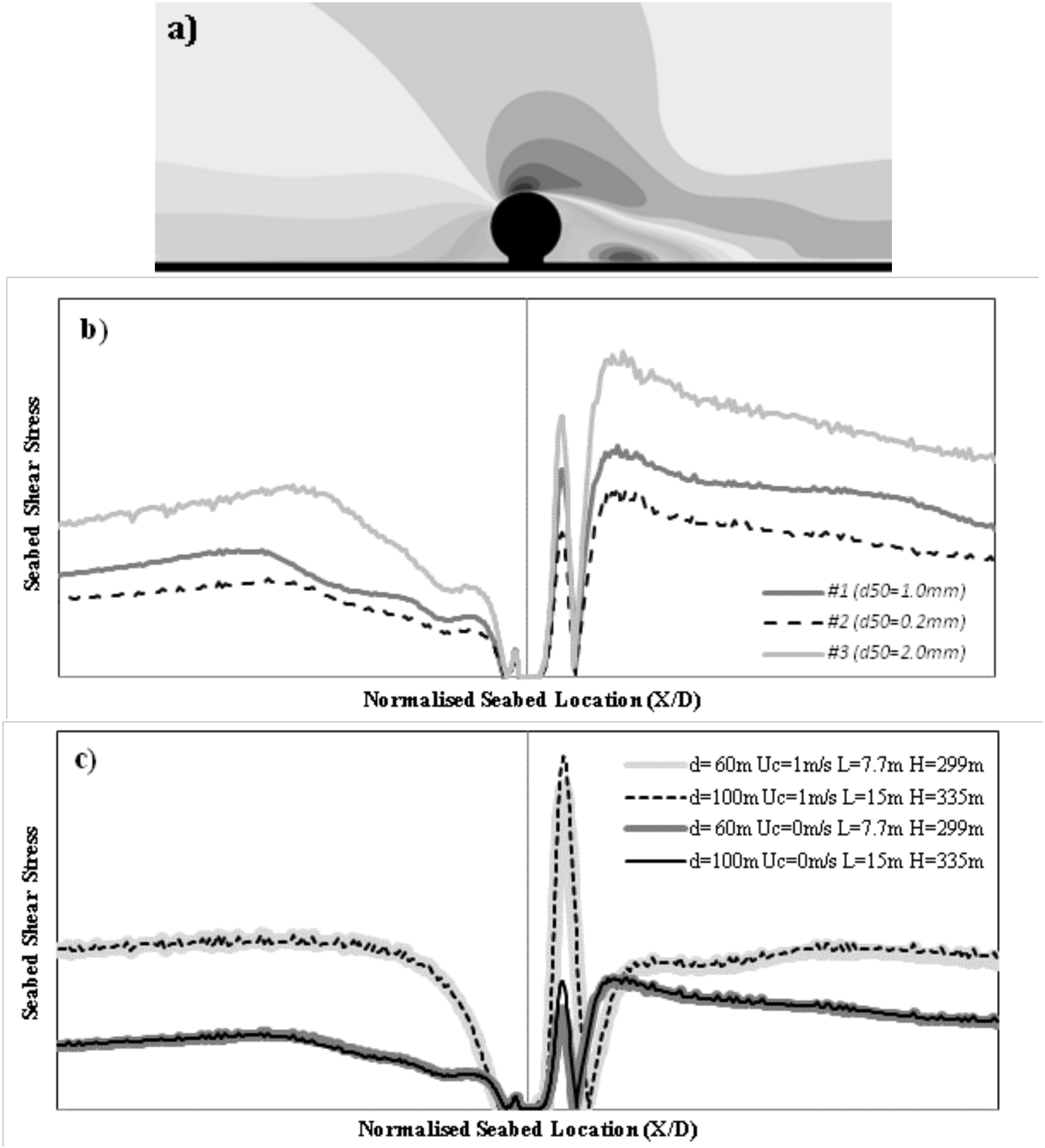

Figure 4 a) X velocity contour plot of a pipe resting on the seabed.
b) Seabed shear stress profiles for varying seabed d_{50} grain sizes.
c) Seabed shear stress profiles for 1m/s wave velocity but with varying water depth, wave length and height ± 1m/s current.

The close-up X velocity contour plot of Figure 4a) is of the base case geometry of a pipe resting on a flat seabed which corresponds to the simulation cases in Figures 4b) & 4c). The three simulation cases of Figure 4b) all had a flow of 1m/s wave velocity and only varied in the seabed roughness parameter by varying average seabed grain size (d_{50}). The smallest average grain size is typical of that found on the North West Shelf of Western Australia and the largest is that of very coarse sand (Soulsby, 1997). It was observed that seabed shear stress approximately doubled when grain size was increased by an order of magnitude over the range tested. This could significantly increase the Shields parameter, and hence sediment transport and rates of scour. The results for d_{50} =1.0mm were from the work of Shen (2011) and are included for comparison. In each case, the maximum seabed shear stress occurred in the turbulent wake flow region down stream of the pipe and can be seen in Figure 4a) where the darker contours correspond to higher X velocities.

In Figure 4c), the two smaller seabed shear stress profiles were both of wave only cases with a 1 m/s wave velocity but differed in water depth (d), wave length (L) and wave height (H). Note that wave length and height were varied to maintain a 1m/s wave velocity as water depth changed. The seabed shear stress for both cases were very similar and only differed by a small margin in the first peak of the turbulent wake flow downstream of the pipe. The two larger seabed shear stress profiles in Figure 4c) were identical cases to the two smaller profiles except they were combined with a 1m/s steady current. The two larger profiles are also very similar but the addition of current has significantly increased the peak and ambient seabed shear stress. There is also a small shift of the stress peaks downstream due to the current.

4. Conclusions and Future Work

The results of this project to date indicate that a combination of waves and currents significantly increase seabed shear stresses as does increasing the d_{50} seabed grain size. This may increase sediment transport as well as scour rates and can be used to refine the clients PSF model. The effects of varying water depth and wave dimensions appear to be minor and may be neglected in the range tested. Further testing of this effect in shallower water depths would increase the range of validity of this observation.

5. References

Cheng, L., Yeow, K., Zhang, Z. & Teng, B. (2009) Three-Dimensional Scour Below Offshore Pipelines in Steady Currents, *Coastal Engineering*, 56, 577-590.

Griffiths, T. (2012) Development of a Novel 2D Pipe-Soil-Fluid Interaction Model for Subsea Pipeline Stability Design, *International Society of Offshore and Polar Engineers,* TPC-0828.

Kazeminezhad, M.H., Yeganeh-Bakhtiary, A., Etemad-Shahidi, A. (2010) Numerical Investigation of Boundary Layer Effects on Vortex Shedding Frequency and Forces Acting Upon Marine Pipeline, *Applied Ocean Research*, 32, 460-470.

Li, F. & Cheng, L. (2001) Effects of Pipeline Sagging on Local Scour Below Pipelines, *20th International Conference of Offshore Mechanics and Arctic Engineering,* Brazil, Pipe-4027, 1-6.

Soulsby, R. (1997) Dynamics of Marine Sands – A Manual for Practical Applications. *Thomas Telford*, London.

Shen, W. (2011) 3D CFD Investigations of Seabed Shear Stresses Around Subsea Pipelines, *The University of Western Australia*.

Sumer, B.M. & Fredsøe, J. (1991) Onset of Scour Below a Pipeline Exposed to Waves, *International Journal of Offshore and Polar Engineers*, **1** (3), 189-193.

Sumer, B.M., Truelsen, C., Sichmann, T. & Fredsøe, J. (2001) Onset of Scour Below Pipelines and Self-burial, *Coastal Engineering*, 42, 313-335.

Xu, M. (2010) CFD Modeling of Seabed Shear Stresses Around Subsea Pipelines, *The University of Western Australia*.